Some Peculiarities of Helicopter Main Rotor Aeroacoustic for Far-Field Observer

Alexander Kusyumov[1*], *Sergey* Mikhailov[1], *Sergey* Kusyumov[1] , *Elena* Romanova[1], and *Georgios* Barakos[2]

[1]Kazan National Research Technical University n.a. A. N. Tupolev (KNRTU-KAI), Kazan, Russia
[2]University of Glasgow, Glasgow, UK

Abstract. Mathematical models for helicopter rotor acoustics are usually based on the Ffowcs Williams–Hawkings (FW–H) equation. The level of rotor noise is determined by geometry (thickness noise) of a flying vehicle and distributed blade loading (loading noise). Initially, the FW-H equation was obtained from Euler's equations and does not depend on the viscosity of flow. In the present work the UH-1H helicopter is considered as a test case for numerical CFD simulation and comparison to experimental data.

1 Introduction

Modern research in rotor noise is based on Computational Aeroacoustics (CAA) and Computational Fluid Dynamics (CFD) to estimate the near-field noise of aircraft.

Tonal noise, generated by a helicopter main rotor, can be described as the sum of two components [1]: thickness and loading noise described by the aerodynamic theory. The thickness noise is determined by the geometry of the rotor blade and the rotor frequency. The thickness noise has a strong in-plane (rotor disk plane) crest directed towards the forward region of the flight.

The term "loading noise" is usually a reference to the harmonic noise from non-impulsive loading sources. Basic loading noise during hover is dominant in a conical region directed 30 to 40 degrees downward from the rotor plane.

Thickness noise and loading noise are described by the linear aerodynamic theory based on the Ffowcs Williams–Hawkings (FW–H) equation [1, 2].

Additional sources, including Blade Vortex Interaction (BVI) noise and High Speed Impulsive (HSI) noise dominate at specific flight regimes.

The HSI noise is associated with shocks and transonic flow around the advancing rotor blades. Including the quadrupole sources in the FW-H equation [1] accounts for nonlinearities in the vicinity of the rotor blade. According to the literature (see, for example, [3]) omission of the quadrupole sources in the FW-H equation leads to inaccurate results for tip Mach numbers higher than 0.7.

To estimate the loading noise requires a CFD solution of the pressure distribution on the blade surface or on of a fictitious permeable surface: using a permeable surface approach is an alternative mathematical formulation that allows for taking into account the HSI noise [4].

As mentioned above the thickness noise level is determined by the rotor blade geometry and the rotor frequency. Analysis of the FW-H equation structure shows that the thickness noise for a far-field observer can be determined without solving the flow equations. The blade geometry parameters of the hovering rotor include aerofoil and blade planform shape, the twist of the blade and the collective angle.

In the present work, estimation of the influence of the collective angle on the thickness noise level of a hovering rotor is considered, using the FW-H equation. Analytical predictions are then compared to CAA results. The main rotor of the UH-1H helicopter is used.

For the numerical modelling, the HMB solver of Glasgow University and ANSYS Fluent13 are used.The sound pressure level is estimated for different observation angles.

2 FW-H equation analysis and solution

The general retarded-time formulation of Farassat, for the observer aeroacoustic pressure p' is commonly referred to as Formulation 1A [1] and is given by the following expression:

$$p'(\mathbf{x},t) = p'_T(\mathbf{x},t) + p'_L(\mathbf{x},t), \quad (1)$$

where $p'_T(\mathbf{x},t)$ and $p'_L(\mathbf{x},t)$ are the thickness and loadimg noise respectively. For a far-field observer the thickness and load noise components can be written as

$$p'_T(\mathbf{x},t) = \frac{1}{4\pi}\int_{f=0}\left[\frac{\rho_0 \dot{v}_n}{r|1-M_r|^2} + \frac{\rho_0 v_n \hat{r}_i \dot{M}_i}{r|1-M_r|^3}\right]_{ret} dS, \quad (2)$$

$$p'_L(\mathbf{x},t) = \frac{1}{4\pi a_0}\int_{f=0}\left[\frac{\dot{p}\cos(\Theta)}{r|1-M_r|^2} + \frac{p\cos(\Theta)\hat{r}_i \dot{M}_i}{r|1-M_r|^3}\right]_{ret} dS. \quad (3)$$

* Corresponding author: postbox7@mail.ru

Here t is the observer time; ρ_0 is the air density; dS is the blade surface element; p is the pressure at emission point; a_0 is the speed of sound; $M_r(\theta,\psi) = \mathbf{M}\cdot\hat{\mathbf{r}}$ is the Mach number in the radiation direction; $r(\theta,\psi) = |\mathbf{x}-\mathbf{y}|$ is the distance between observer and source;$\mathbf{x}$ is the observer position vector, and $\mathbf{y}$ is the source position vector; $v_n(\theta,\psi) = \mathbf{v}\cdot\mathbf{n}$ is the local normal velocity of source surface; $\theta(\mathbf{y})$ is the blade pitch angle; ψ is the blade azimuth angle. The above expressions also include $\cos(\Theta) = \mathbf{n}\cdot\hat{\mathbf{r}}$, where Θ the local angle between the normal vector $\mathbf{n}$ to the emission surface, and the radiation direction $\hat{\mathbf{r}}$ at the time of emission. A dot over variables is used as a symbol of differentiation with respect to time of the emission source. The subscript *ret* stands for the retarded time with the integration evaluated over the emission surface. For solution of the FW-H equation numerical (CFD) simulation results are used for the acoustic pressure at the source determination.

For simplicity, a rotor blade without twist and coning is considered. In this case for the hovering rotor $\theta(\mathbf{y}) = \text{const}$. From the physical properties of flow (invariance of flow with the respect to the blade azimuth angle ψ) it follows that for hover $\dot{v}_n = 0$ and expression (2) can be written as

$$p_T'(\mathbf{x},t) = \frac{\rho_0}{4\pi}\int_{f=0}\left[\frac{v_n\dot{M}_r}{r|1-M_r|^3}\right]_{ret} dS. \qquad (3)$$

For a far-field observer, it can be accepted that: $r(\theta,\psi)\approx const = d$, and $M_r(\theta,\psi) \approx M_r(\psi)$. These lead to:

$$p_T'(\mathbf{x},t) = \frac{\rho_0}{4\pi d}\int_{f=0}\left[\frac{v_n(\theta)\dot{M}_r(\psi)}{|1-M_r(\psi)|^3}\right]_{ret} dS. \qquad (4)$$

Expression (4) can be written as

$$p'_T(t,\mathbf{x}) = \frac{\rho_0}{4\pi d}\int_{f=0}[V_n(\theta)]_{ret} dS. \qquad (5)$$

Here, the normal vector to a surface element dS is determined by:

$$V_n(\theta) = \frac{v_n(\theta)\dot{M}_r(\psi)}{|1-M_r(\psi)|^3}.$$

Entry (5) can be considered as the flux [5, 6] of a vector field $\mathbf{V}(\theta)$ through the blade surface $f = 0$:

$$p_T'(\mathbf{x},t) = \frac{\rho_0}{4\pi d}\int_{f=0}[\mathbf{V}(\theta)]_{ret}\cdot d\mathbf{S}, \qquad (6)$$

where $d\mathbf{S}$ is an oriented blade surface element.

The blade surface element $d\mathbf{S}$ can be determined as $d\mathbf{S} = d\mathbf{s}dl$, where $\mathbf{s}\in\boldsymbol{\Sigma}$ is the aerofoil coordinate at a local blade section and l is a spanwise coordinate. It is evident that for a blade with similar tip and root aerofoil's the integral (6) can be written as

$$p_T'(\mathbf{x},t) = \frac{\rho_0}{4\pi d}\int_L \{\oint[\mathbf{V}(\theta)]_{ret}\cdot d\mathbf{s}\}\, dl.$$

The line integral around the closed loop is the Flux induced by $\mathbf{V}$ across (FA) a closed curve $\boldsymbol{\Sigma}$:

$$\text{FA}\ \boldsymbol{\Sigma} = \oint[\mathbf{V}(\theta)]_{ret}\cdot d\mathbf{s} = \oint[\mathbf{V}(\theta)]_{ret}\cdot\mathbf{n}_{\boldsymbol{\Sigma}} ds. \qquad (7)$$

Here $\mathbf{n}_{\boldsymbol{\Sigma}}$ is a unit normal vector to the curve $\boldsymbol{\Sigma}$. For the periodical flow around the hover rotor the integral (7) can be considered in 2D space with local aerofoil coordinates (y,z):

$$\mathbf{FA}\ \Sigma = \oint[\mathbf{V}(\theta)]_{ret}\cdot\mathbf{n}_{\boldsymbol{\Sigma}} ds.$$

In 2D space, the continuous velocity is:

$$\mathbf{V}(\theta) = V_y(\theta,y,z)\,\mathbf{j} + V_z(\theta,y,z)\,\mathbf{k},$$

where $\mathbf{j}$ and $\mathbf{k}$ are the unit vectors along the y and z coordinates, and V_y and V_z are components of the vector $\mathbf{V}$. For the smooth curve $\boldsymbol{\Sigma}$:

$$s(\varphi) = y(\varphi)\mathbf{j} + z(\varphi)\mathbf{k},\ \varphi\in[0,2\pi]. \qquad (8)$$

(angles φ and θ are determined with the same coordinate system). Then the vector $\mathbf{V}(\theta)$ can be presented as

$$\mathbf{V}(\theta) = V_y(y(\varphi+\theta),z(\varphi+\theta))\mathbf{j} + V_z\big(y(\varphi+\theta),z(\varphi+\theta)\big)\mathbf{k}. \qquad (9)$$

Using (9) the vector of local normal $\mathbf{n}_{\boldsymbol{\Sigma}}$ can be written as:

$$\mathbf{n}_{\boldsymbol{\Sigma}} = \frac{1}{|s'(\varphi)|}\left(\frac{dz}{d\varphi}\mathbf{j} - \frac{dy}{d\varphi}\mathbf{k}\right),$$

and this leads to the conclusion that

$$\text{FA}\ \boldsymbol{\Sigma} = \oint[\mathbf{V}(\theta)]_{ret}\cdot\mathbf{n}\, ds = \oint\left[V_y(\theta)\frac{dz}{d\varphi} - V_z(\theta)\frac{dy}{d\varphi}\right]_{ret} d\varphi.$$

For hover, the pitch angle θ is constant and one must introduce a new angular variable $\bar{\varphi} = \varphi + \theta$:

$$\text{FA}\boldsymbol{\Sigma} = \oint[\mathbf{V}(\theta)]_{ret}\cdot\mathbf{n}\, ds = \oint\left[\bar{V}_y|_{\theta=0}\frac{dz}{d\bar{\varphi}} - \bar{V}_z|_{\theta=0}\frac{dy}{d\bar{\varphi}}\right]_{ret} d\bar{\varphi}, \qquad (10)$$

where $\bar{V}_y = V_y\big(y(\bar{\varphi}),z(\bar{\varphi})\big)$ and $\bar{V}_z = V_z\big(y(\bar{\varphi}),z(\bar{\varphi})\big)$.

From (10) it follows that **FA Σ** does not depend on the pitch angle θ. This implies that the thickness noise $p_T'(\mathbf{x},t)$ value does not depend on pitch.

The mathematical model (1)–(3), corresponds to the classical impermeable formulation of FW–H equation. In this case, the source surface $f = 0$ corresponds to the blade surface. This model, for high blade tip Mach numbers, usually gives under predicted values of the noise level. Nevertheless the classic FW–H formulation was used in recent publications for relatively low values of the blade tip Mach numbers (see reference [7], for example). Then, the acoustic pressure (based on the Formulation 1A) can be modified with empirical adjustments, based on the radiation Mach number M_r. In this work the radiation vector $\hat{\mathbf{r}}$ ofthe source – observer distance projected to the shaft – observer direction is used instead of the source-observer distance. This is applied to the far-field thickness noise.

As the rotor blade is characterized by a complex motion in the computer program it is assumed that the blade is a rotating rigid body.

The employed algorithm is similar to the algorithm, described in [1]. The first stage of FW-H solution is to divide the rotor blade surface in a number of panels. Integration over each panel is approximated using the value at its centroid.

Rotation matrices and angular velocity vectors are used to describe the blade rotation and the effects of pitch, cone and rotor disc tilt angles. Positions and velocities of points are determined in a blade-fixed stationary frame by combining the matrices/vectors with rigid body surface relations for rotating reference frames.

The summed effect of all the panels at the observer location gives the acoustic pressure time history. The algorithm was implemented in the in-house H-FWH computer code.

3 CFD Modelling

Numerical simulations were conducted for the 1/7 scale UH-1H rotor. The geometry of the full-scale UH-1H blade is presented in Table 1 [8]. Since temporal and spatial periodicity is assumed for the flow, the computational grid was generated for a single rotor blade (with appropriate periodic boundary conditions). For this two-bladed rotor, the computational domain is a half of a cylinder. The multi-block topology used in this paper can be seen in Figure 1. C-type blocking is used around the blade. The structured and multi-block computational grid consisted of 88 blocks and 8.4 million cells. Along the aerofoil surface, 218 points are located with a concentration near the leading and trailing edges. Normal to the surface, the first cell size was 10^{-5} of the blade's chord length and the cell aspect ratio was less than 1.2.

Table 1. UH-1H operational characteristics.

Parameter	Value
Number of blades N	2
Rotor radius $2R$, m	14.63
Rotor solidity σ	0.0464
Blade chord$c$, m	0.53
Blade airfoil	NACA 0012
Blade twist (root to tip), deg	-10.9
Max gross weight W, N	43000

The multi-block topology used in this paper can be seen in Figure 1. Around the blade, C-type blocking topology is used.

The flow fields around the UH–1H helicopter rotor in hover were numerically simulated by solving 3D steady Reynolds-Averaged Navier-Stokes (RANS) equations.

The "periodic" boundary condition provides the periodicity of the flow around the blade.

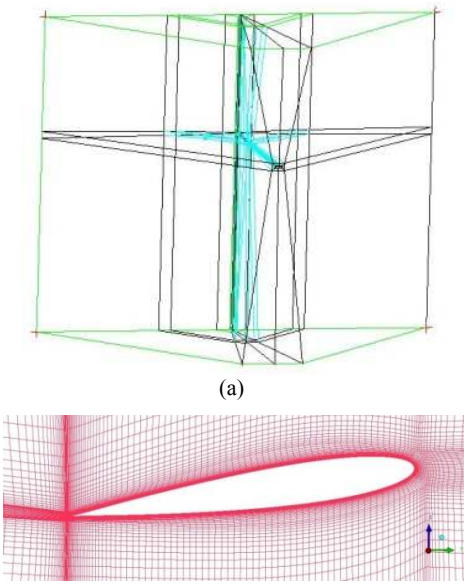

(a)

(b)

Fig. 1. Multi-block topology (a) and mesh section (b).

For HMB the "source-sink" boundary conditions [9] were used at all surfaces of the computational domain apart from the symmetry plane. The inflow (W_{in}) and outflow (W_{out}) velocities were obtained from momentum theory according to the expressions:

$$W_{in}(x,y,z_u) = -\frac{U}{8}\sqrt{C_T}\left(\frac{R}{L}\right)^2; \quad W_{out} = -U\sqrt{C_T}.$$

Here U is the speed of the blade tip; L is the distance between the rotor centre and an arbitrary (x,y,z_u) point on the upper surface z_u=const of the computational domain. The thrust coefficient C_T is determined as

$$C_T = \frac{T}{\pi R^2 q_{tip}},$$

where q_{tip} is the dynamic pressure at the blade tip and T is the rotor thrust, obtained after iterative computations. The rotor thrust coefficient C_{TW} (under the condition T=W) is first used as an initial guess and then the thrust coefficient value C_T is recomputed using successive approximations.

Similar boundary conditions with some differences at the bottom part of modelling domain were used for the HMB and Fluent solvers: in Fluent for the bottom part of the computational domain, the «pressure-outlet» boundary condition was assigned.

The flow conditions and the values of the trust coefficient obtained with HMB and Fluent are presented in Table 2. A collective pitch angle $\theta_{0.75}$ was chosen according to approximate trimming methods [10]. The values $\bar{W}_{in}$ of averaged on the upper part of the computational domain used for computations in both HMB and Fluent are shown in Table 2. Some discrepancy between HMB and Fluent results can be explained, by the different type of boundary conditions at the upper and bottom parts of the computational domain: in Fluent $W_{in} = \bar{W}_{in} = const,$ and for the bottom part of the

computational domain, the «pressure-outlet» boundary condition was assigned.

Table 2. Conditions for computations.

Parameter	Value
Collective pitch, $\theta_{0.75}$	7°
Tip Mach number, M_{tip}	0.8
Tip Reynolds number, Re	9.5×10^6
Thrust coefficient (for $T=W$), C_{TW}	0.0055
Inflow velocity (HMB), $\bar{W}_{in}$	0.201 m/s
Inflow velocity (Fluent), $\bar{W}_{in}$	0.2 m/s
Thrust coefficient (HMB), C_T	0.00577
Thrust coefficient (Fluent), C_T	0.0054

Simulations were conducted with the k-ω SST turbulence model. Some simulation results are shown in Figure 2 (see also reference [11]).

(a)

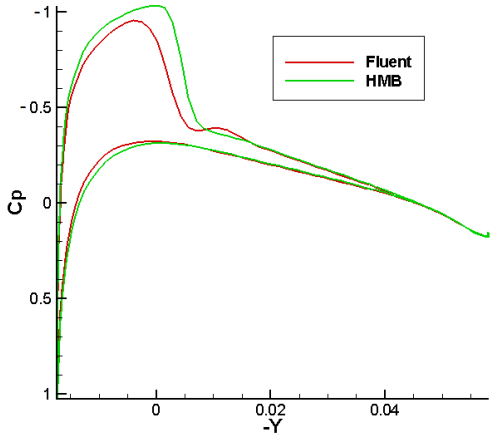

(b)

Fig. 2. Visualization of vortex cores with the Q criterion (a); distribution of the pressure coefficient Cp at the blade section $\bar{r} = r/R$ = 0.95 (b).

Figure 2(a) shows the regions of high vorticity magnitude visualized with the Q criterion. Some discrepancy between pressure coefficient distribution obtained in HMB and Fluent codes in Figure 2(b) is consistent with the difference between the predicted values of the thrust coefficient (Table 2).

The geometry of the rotor blade, blade surface pressure distribution and the conditions of the computations were used to estimate the sound propagation via the FW-H equation.

4 FW-H equation solutions

Figure 3 presents the results of numerical simulation and experiments [8] for a far-field observer located at the rotor disc plane on the distance of 3R=3.135 m away from the rotor.

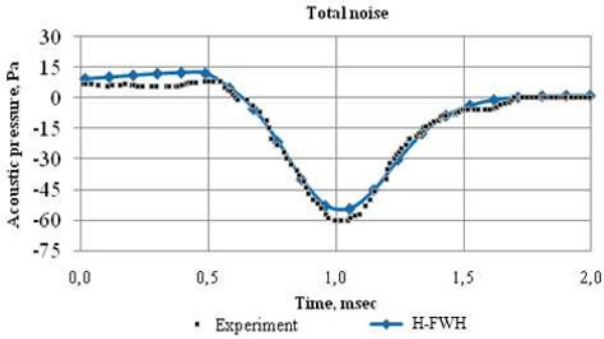

Fig. 3. Comparison of CFD and experimental data for a far-field observer at 3R on the rotor disk plane.

The total noise predicted by the H-FWH code for an observer located on the rotor plane is in good agreement with the measurements.

Figures 4 and 5 show the thickness and total noise pressure vs the observation time for the different collective $\theta_{0.75}$ (3.7, 7 degrees) and observation Θ (0, 15 degrees) angles.

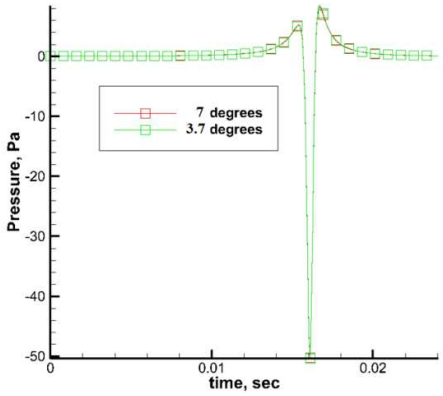

(a)

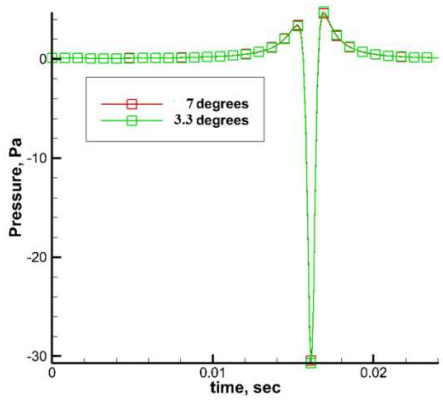

(b)

Fig. 4. Thickness noise predicted for different collective pitch, $\theta_{0.75}$ and observation angles:
Θ=0 degrees (a), and Θ=15 degrees (b).

From Figure 4 it follows that the thickness noise level does not depend on the collective angle values, corresponding to a conclusion following from the expression (10).

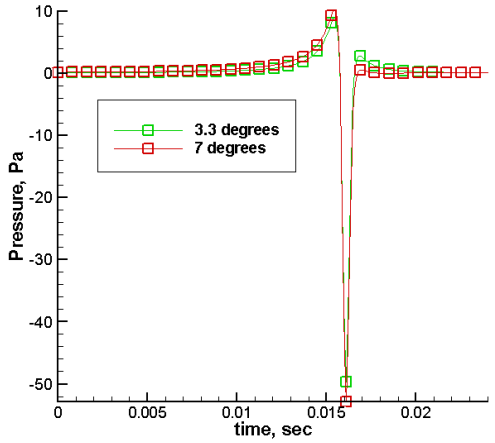

(a)

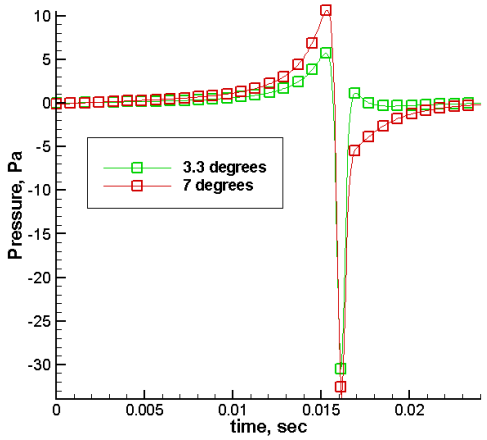

(b)

Fig. 5. Total noise predicted for different collective pitch, $\theta_{0.75}$ and observation angles: Θ=0 degrees (a), and Θ=15 degrees (b).

Unlike the thickness noise the load noise values depends on the pitch angle. For this reason, the total noise pressure depends on the pitch angle also (see Figure 5).

5 Conclusion

In this work, the influence of the collective angle on the thickness noise level of a hovering rotor is considered using the FW-H equation. Theoretically was shown that the thickness noise value does not depend on the pitch angle value.

The total rotor noise was considered as a sum of the thickness and load noise based on the linear formulation of aeroacoustic equations. To determine the near-field flow parameters for the UH-1H rotor in hover the in-house HMB CFD code was used.

The classic FW–H formulation was used for relatively low values of the blade tip Mach number. Then, the acoustic pressure (based on the Farassat Formulation 1A) was modified with empirical adjustments.

This work was supported by the grant No. 9.1577.2017/4.6 of the Ministry of Education and Science of the Russian Federation.

References

1. K. S. Brentner, F. Farassat, Progress in Aerospace Sciences, **39** (2003)
2. K. S. Brentner, NASA-TM-111251 Report, NASA Langley Research Center, Hampton, VA (1996)
3. A. S. Lyrintzis, Aeroacoustics, **2**, no. 2 (2003)
4. P. di Francescantonio, Journal of Sound and Vibration, **202**, 4 (1997)
5. M.R. Spiegel; S. Lipschutz; D. Spellman, *Vector Analysis* (McGraw Hill, 2009)
6. R. Courant and F. John, *Introduction to calculus and analysis* (Volume II, Springer-Verlag, 1961)
7. K. Sharma, K. S. Brentner, *AHS 72nd Annual Forum*, *West Palm Beach, Florida* (2016)
8. F.H. Schmitz and Y.H., Yu, NASA Technical memorandum 84390 (1983)
9. N. A. Mohd, G. N. Barakos, *RAeS Aerodynamics Conference*, *University of Bristol, UK* (2010)
10. J. Seddon, *Basic helicopter aerodynamics*, (BSP professional books, 1990)
11. A. Kusyumov, S. Mikhailov, A. Batrakov, S. Kusyumov, G. Barakos, *EPJ Web Conf.*, **143** (2017)